A parametric study of the repeatability of 3D printed LEGO®-like mechanical couplings

by
Rebecca Kurfess

Submitted to the
Department of Mechanical Engineering
in Partial Fulfillment of the Requirements for the Degree of

Bachelor of Science in Mechanical Engineering

at the

Massachusetts Institute of Technology

June 2017

Signature of Author: Signature redacted

Department of Mechanical Engineering

May 19, 2017

Certified by: Signature redacted

Anastasios John Hart

Associate Professor of Mechanical Engineering

Signature redacted Thesis Supervisor

Accepted by: _____

Rohit Karnik

Associate Professor of Mechanical Engineering

Undergraduate Officer

A parametric study of the repeatability of 3D printed LEGO®-like mechanical couplings

by

Rebecca Kurfess

Submitted to the Department of Mechanical Engineering
on May 19, 2017 in Partial Fulfillment of the
Requirements for the Degree of
Bachelor of Science in Mechanical Engineering

Abstract

Parts made using Additive Manufacturing (AM) are limited in size to the build area of the 3D printer being used. Embedded elastically averaged locators can be used to join AM parts into assemblies, resulting in a piece larger than the build area, yet the design and placement of these locators must enable sufficient accuracy and repeatability of the couplings. In this thesis, locator design was formulated and verified using contact area, interference, and stiffness of the couplings as the design variables. A LEGO®-like coupling design was printed out of ABS on an Afinia H480 Fused Deposition Modeling (FDM) printer and measured with a ZEISS MICURA Coordinate Measuring Machine. The accuracy of each coupling was determined by measuring the radial misalignment between the base and the top of the coupling, and the repeatability of each coupling was determined by calculating the standard deviation of the radial misalignment after de-coupling and re-coupling five times. The couplings were displayed accuracy on the order of 10 μm and repeatability on the order of 1 μm. Varying interference, contact area, and stiffness had a statistically insignificant effect of accuracy. Varying interference had a statistically insignificant effect on repeatability, increasing contact area increased repeatability by 0.75 μm, or 15%, and increasing increased repeatability by 0.57 μm, or 12%.

Thesis Supervisor: Anastasios John Hart
Title: Associate Professor of Mechanical Engineering

ACKNOWLEDGEMENTS

To my dad, Tom Kurfess: You are the reason I fell in love with engineering, and you inspire me to be a better engineer every day. Without your guidance and support, none of this would have been possible. Thank you for the advice, the time you took to edit each revision of my thesis, and all of the hours you spent on the phone with me discussing every topic covered in this thesis.

To my mom, Adriana Kurfess, and my brother, Greg Kurfess: Thank you for listening to me think out loud and for helping me print all of my couplings. Greg, you are going to be a great engineer!

To Cyndia Cao, Crystal Owens, and Ryan Penny: Thank you for answering all of my engineering questions and giving me advice on everything from how to print a better LEGO® to how to improve my diagrams.

To Max Praniewicz, John Miers, Steven Sheffield, and the faculty and staff at Georgia Tech: Thank you for letting me use your CMM and tomography machine and for taking time out of your busy schedules to teach me how to use them.

To Professor John Hart: I discovered just how incredible LEGOs® are from you in 2.008, and I am so grateful to have had the opportunity to continue to learn about them with your guidance.

Table of Contents

Acknowledgements 5

Introduction 11

Background 13

Additive Manufacturing 13

Couplings 20

Factorial Design of Experiments 22

Experimental Apparatus and Procedure 24

Results and Discussion 35

Accuracy 35

Repeatability 36

Contact Points 38

Discussion 39

Conclusions and Recommendations 41

Bibliography 43

List of Figures

Figure 1. The a) base and b) top of the coupling optimized for use in AM parts. 11
Figure 2. Layers of material in an FDM part. 16
Figure 3. Overview of the setup for the original patent on the FDM process. 17
Figure 4. Support structures allowing an overhanging part to be printed with FDM. 18
Figure 5. Two cylinders printed with different orientations 19
Figure 6. Afinia H480 3D printer. 20
Figure 7. Three-ball three-groove kinematic coupling. 21
Figure 8. Lego building blocks. The a) pegs on top of one brick mesh with the b) thin web on the bottom of another brick 22
Figure 9. The renderings of the a) base and b) top of the coupling and the c) base and d) top of the printed coupling. 25
Figure 10. The a) rendering of the coupled assembly and b) 3D printed coupled assembly. 26
Figure 11. The a) small web diameter of 6.25 mm, b) large web diameter of 6.51 mm, c) short peg height of 1.5 mm, and the tall peg height of 2.2 mm. 27
Figure 12. The coupling with a) no relief cuts and b) four relief cuts per web diameter. 27
Figure 13. Print orientation and direction, indicated by the arrow. 31
Figure 14. The a) modelled experimental setup and b) experimental setup. 31
Figure 15. The path taken by the CMM to around the a) base of the coupling and b) top of the coupling to determine its location in space and dimensions. 32
Figure 16. The distance between the centers of the base and top of the coupling used to determine misalignment. 33
Figure 17. The ink distribution on traditionally manufactured LEGO® building block. The circular web on the top of the coupling, boxed in red, shows inked spots 90° apart from each other, indicative of the locations where the ink-covered pegs of the base coupling, boxed in blue, made contact 34
Figure 18. The points at which the pegs contact the web on a traditionally manufactured LEGO®. 34
Figure 19. Accuracies of the couplings with contact area, interference, and stiffness varied, with 95% error bars 36

Figure 20. Repeatabilities of the couplings with contact area, interference, and stiffness varied, with error bars indicating 95% error of the fixturing setup. 37
Figure 21. Assembled coupling as imaged with tomography, with contact points circled in red. 38
Figure 22. The a) base of the coupling, with ink applied to the pegs, and b) the top of the coupling, with the areas of ink transfer circled in red..... 39

List of Tables

Table 1. Common additive manufacturing systems..... 14
Table 2. Comparison of prices and build volumes of MakerBot printers..... 16
Table 3. Sample factorial DOE testing the impact of 3 factors, each with two levels, a low (-1) and a high (+1)..... 23
Table 4. Coupling variations..... 29
Table 5. Misalignment averages and standard deviations for each trial..... 35

INTRODUCTION

Additive Manufacturing (AM) processes are being utilized at an increasing rate because the complexity of the parts has little to no impact on their cost. In order to effectively utilize AM in more advanced manufacturing applications, the ability to precisely locate the AM part (precision locating) is needed. This would enable accurate assembly of AM components, as well as accurate fixturing of AM parts for subsequent machining and finishing operations. Incorporation of kinematic couplings in AM parts can address this need, but the use of kinematic couplings results in limited load capacity and system stiffness as applied loads are concentrated over a small area of contact [1]. Elastically averaged couplings, which operate by over-constraining the coupled bodies using a large number of relatively complaint pieces, permit higher stiffness and lower local stress [2].

For this research, a Lego®-like coupling, shown in Figure 1, was used as the initial design for the coupling, and the geometry of the coupling was designed for use as an AM coupling. Stiffness, contact area, and interference of the coupling were then varied by adding reliefs, varying the height of the pegs (boxed in green, Figure 1) and varying the diameter of the web (boxed in blue, Figure 1).

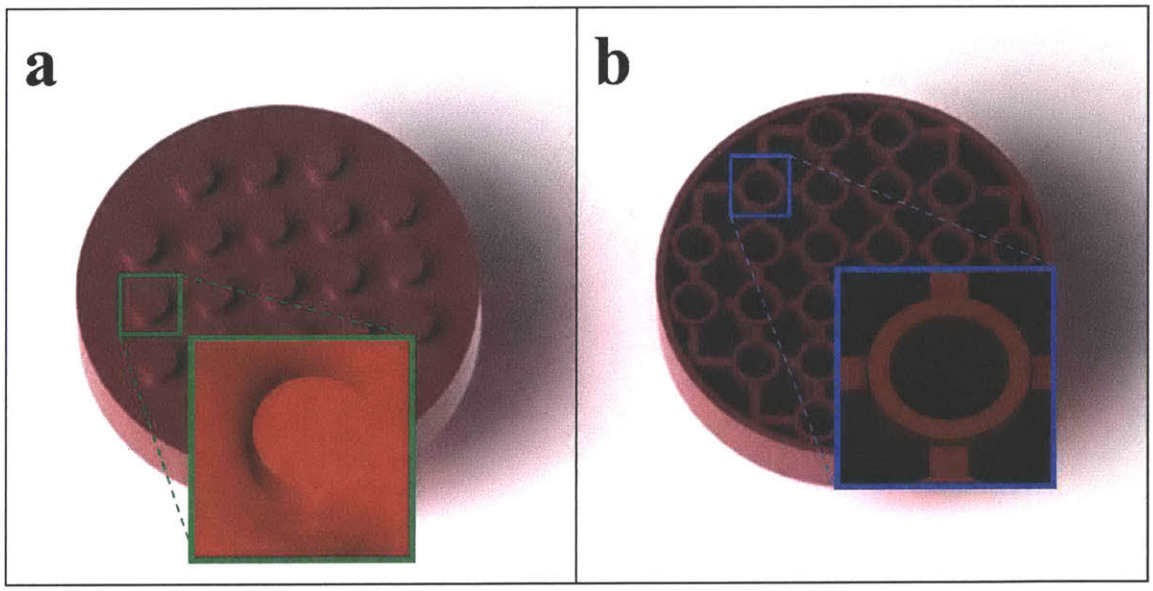

Figure 1. The a) base and b) top of the coupling designed for use in AM parts.

To determine the accuracy and repeatability of each coupling variation, the base of the coupling was fixed and its center location was measured. The top of the coupling was then coupled and de-coupled multiple times, and the radial misalignment between the top and base was measured each time. The average radial misalignment for each coupling was used to characterize the accuracy of the coupling, and the standard deviation of all the radial misalignment measurements for each coupling was used to characterize the repeatability of the coupling. A more detailed explanation of the procedures used is given in the ensuing text.

Next, a background discussing additive manufacturing and coupling design is presented. Then, the experimental apparatus and procedure used to measure the misalignment of the couplings is described, and the accuracy and repeatability results of the couplings are discussed. Conclusions based on the accuracy and repeatability results of each coupling are drawn, and future recommendations are made based on these conclusions.

BACKGROUND

Additive Manufacturing

Two major categories of manufacturing include additive and subtractive manufacturing. Subtractive manufacturing refers to any process that begins with a large block of material and produces a part by removing unwanted material. Subtractive manufacturing processes include milling, turning, and cutting. Additive manufacturing (AM), on the other hand, refers to any process that is used to produce objects by adding material where there was previously none, including 3D printing. There are many different AM processes, utilizing various materials, technologies, and processes. Table 1 lists several common AM processes and describes each process's method for producing the layers necessary to construct a 3D part.

Table 1. Common additive manufacturing systems [3].

AM System	Description
Binder jetting	A bonding agent is extruded onto a powdered material, binding the granules together
Directed energy deposition	Focused thermal energy is used to fuse materials by melting as they are being deposited
Material extrusion	Material is selectively dispensed through a nozzle or orifice
Material jetting	Droplets of build material are selectively deposited
Powder bed fusion	Thermal energy selectively fuses regions of a powder bed
Sheet lamination	Sheets of material are bonded to form an object
Vat photopolymerization	Liquid photopolymer in a vat is selectively cured by light-activated polymerization

Each AM process varies in material type, material cost, printer cost, production time, part surface finish, and structural integrity of parts, so each system is used for different purposes. For example, lower-cost Fused Deposition Modeling (FDM) printers, which utilize a material extrusion process to produce parts by extruding heated plastic through a nozzle, typically produce polymer parts with a lower production time than many other systems but require support structures for parts with overhangs, holes, or other similar geometries, so an FDM printer is used for prototyping lower-complexity, lower-cost, and lower-strength parts. On the other hand, SLS printers are much more expensive, but SLS parts do not typically require support structures, so an SLS system would be used for producing high-complexity, industrial-grade parts. Overall, the end purpose of the part must be considered when choosing an AM system to produce the part.

AM parts used for prototyping can have lower strength and poorer surface finish, while AM parts used in product that are distributed to customers must have a higher structural integrity and surface quality, and will therefore cost more.

AM technology has been commercially available for several decades, and, until recently, has been used mainly as tools for design and prototyping. As the technology develops and becomes more affordable, AM has received more attention due to its potential to transform the manufacturing industry. Its use as a design and prototyping tool has already decreased the time and cost necessary for the iterative design process, allowing new products to be designed and validated at a reduced cost in a shorter period of time. AM technology is beginning to be used to construct functional parts that are the end product being sent to consumers. Through AM, manufacturers have the ability to produce customized or complex parts with no added cost, reduce the amount of waste material created during the production process, manufacture parts outside of a factory setting, and make their production more on-demand, lowering the need for large product inventories and spare parts [4]. This ability is of particular interest to fields where products are either highly customized, such as prosthetics used in the medical field, and fields where lower quantities of products are manufactured, such as a rockets in the aerospace field. Although there is interest in employing AM fabricated products in the field because of the ability to customize and add complexity with ease, the use of AM in manufacturing is not widespread because of several disadvantages of parts produced by AM.

Unlike subtractively manufactured parts that typically consist of a single material machined to a target geometry, AM parts consist of many layers of material, as seen in Figure 2. These layers result in material properties that are less desirable that classically manufactured parts. For example, Shubham et al. determined that an FDM part has an ultimate tensile strength between 1.5 and 2 times less than an injection molded part of the same material and a Rockwell hardness between 1.1 and 1.9 times less than an FDM part of the same material, depending on the layer thickness of the FDM part [5]. The parts are also anisotropic because they are made of multiple layers stacked in the print direction, so the properties of AM parts depend on the part orientation.

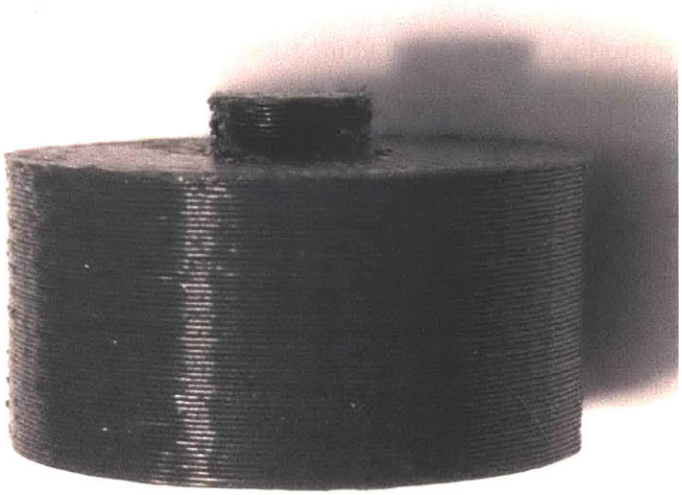

Figure 2. Layers of material in an FDM part.

As with most manufacturing systems, AM part volume is limited by the print volume of the printer in use. The print volume is dependent on the size of the printer, so the maximum part size a consumer is able to produce is dependent on printer volume and, ultimately, cost. In general, printer size and print volume scale with printer cost. Table 2 compares three MakerBot printers, showing their price on dell.com and their print volume. The printer with the largest print volume is approximately 5 times more expensive than the printer with the smallest print volume, but even the largest printer is unable to produce parts greater than 2590 cubic inches in size.

Table 2. Comparison of prices and build volumes of MakerBot printers [6] [7]

Printer	Build Volume (Cubic Inches)	Price (Dollars)
MakerBot Replicator Mini+	100 (4x5x5)	$1299
MakerBot Replicator+	575 (11.6x7.6x6.5)	$2499
MakerBot Replicator Z18	2375 (11x12x18)	$6499

The couplings optimized for precision locating of AM parts in this research were fabricated using the FDM process. The FDM method of depositing multiple layers of solidifying material to create a 3D object was invented by S. Scott Crump in 1989, with a patent, shown in Figure 3, being granted in 1992 [8]. Stratasys commercialized FDM shortly afterwards, but the technology remained expensive until 2009 when the patent expired and some FDM printers became available for hundreds of dollars, instead of thousands of dollars. The printers required to produce high-quality parts still cost several thousand dollars, but the FDM technology is available at a lower cost, and printers that cost a few hundred dollars are becoming a commodity.

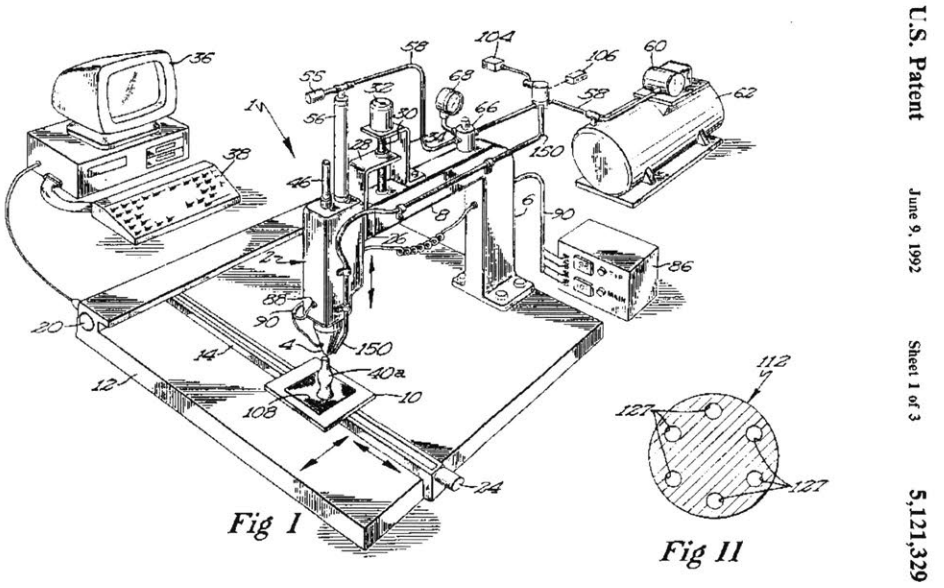

Figure 3. Overview of the setup for the original patent on the FDM process, including a computer to drive the process with computer aided design (CAD), a head that can move in the z-axis to dispense material, and a platform that can move in the x- and y-axes [8].

Crump also invented the process of using supports when printing with FDM [9]. As shown in Figure 4, support structures allow objects with overhangs to be suspended in space during the printing process. The support structures are made either of the same material as the part, printed such that they are weaker and easy to break off, or of a

different material, such as a soluble support material that can be dissolved once the part is completed.

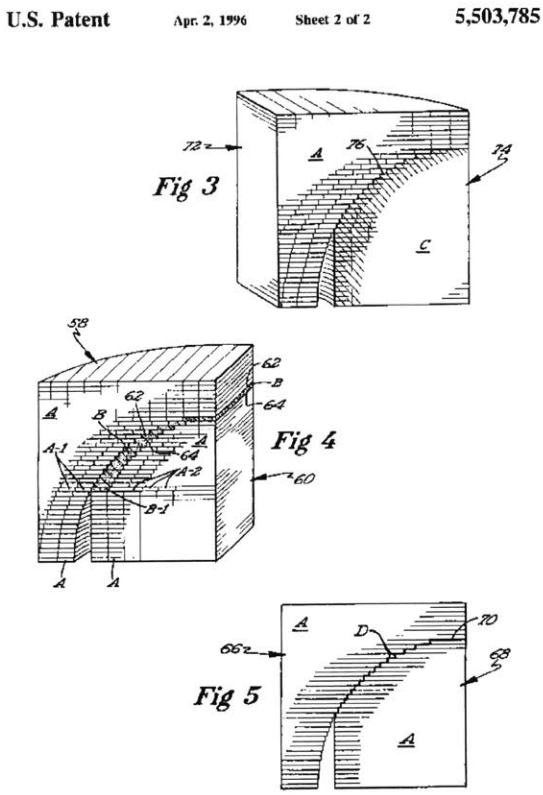

Figure 4. Support structures allowing an overhanging part to be printed with FDM [9].

FDM printers generally rely on computer programs to process a CAD model, which consists of slicing and orienting the part, generating support structures if necessary. The print orientation of an FDM has a significant impact on the part quality and properties, as the direction of the layers impacts surface finish, strength, and accuracy of a part. Different print orientations can also impact the support structures necessary to print a part. For example, the two cylinders shown in Figure 5 were printed based on the same CAD model, but the cylinder on the right was printed rising in the radial direction, which decreased the surface finish quality, added a flat surface to the bottom of the print, and required support structures to print successfully.

Figure 5. Two cylinders printed with different orientations [10]

The Afinia H480 3D Printer used to fabricate the couplings, shown in Figure 6, prints using the FDM process. The printer software processes a stereolithography (STL) file into slices and orients the part onto the printing plate. The plate is preheated to prevent a large temperature difference between the heated filament and the plate, which could cause warping and distortion. Then the heated ABS plastic filament is extruded and deposited via an extrusion nozzle. The extrusion nozzle and the print plate move in the lateral directions while the heated ABS filament is extruded in a pattern pre-determined by the printer software. During this operation, the nozzle is fixed vertically, generating a single planar layer of the part. Following the completion of an entire layer, the print plate is moved down one layer thickness in the vertical direction and a subsequent layer is produced. According to the system's specifications, the Afinia H480 is capable of producing parts up to 5 cubic inches in volume and has an output that is accurate to within 0.15mm. Parts printed on the Afinia H480 typically have 30% of the strength of injection molded parts [11].

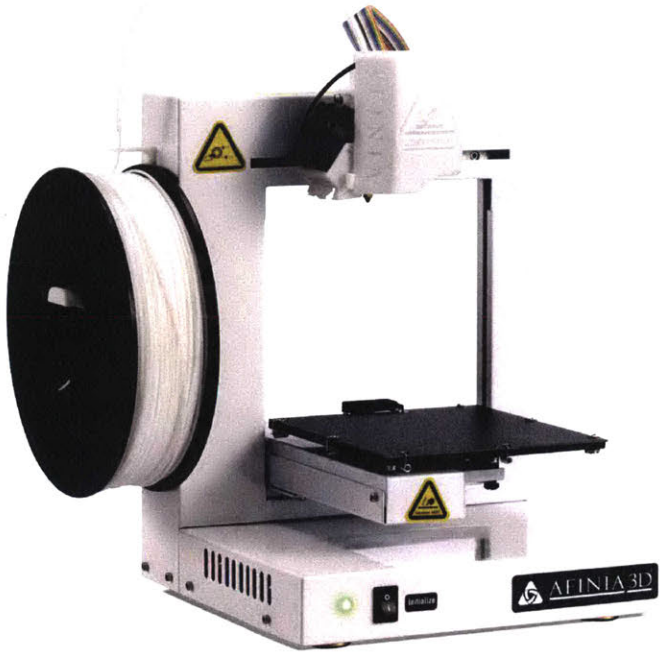

Figure 6. Afinia H480 3D printer [11].

Couplings

Couplings allow one component to be located with respect to another, so they must contain some mechanism that enables one half of the coupling to be accurately located on the other. Kinematic couplings comprised of three balls and three grooves, shown in Figure 7, are often used for precision location because they constrain all 6 degrees of freedom using 6 points of contact, so the component is theoretically perfectly constrained and precisely located. In reality, the point contacts deform into a Hertzian contact ellipses under high loads. Because the area of contact is small, contact stresses in kinematic couplings are often high.

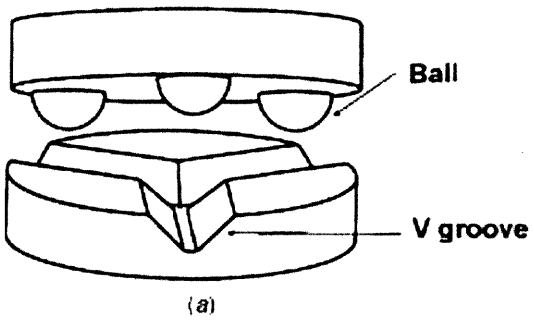

Figure 7. Three-ball three-groove kinematic coupling [12].

Elastic averaging denotes a subset of coupling types where accuracy is derived from the averaging of error over a large number of contact surfaces. The repeatability and accuracy obtained with elastically averaged couplings are generally not as high as those obtained with kinematic couplings, but the design of elastically averaged systems yields higher stiffness and lower local stress [13]. Studies have shown that the repeatability of a three-ball, three-groove kinematic coupling with grooves made of cast iron and balls made of silicon nitride preloaded with 45 kN is on the order of 0.36 μm, while the repeatability of LEGO® building blocks, which are elastically averaged couplings, is on the order of 0.5 μm - 1 μm [2,14,15].

The principles of elastic averaging are used in many different coupling designs, one of the most well-known being the LEGO® building block, shown in Figure 8. LEGO® building blocks are coupled when the projecting cylinders, or pegs, on the top of one brick interface with the thin web on the bottom of another brick to create a small interference fit. The forced compliance causes the pegs and web to deform and then return elastically when the blocks are separated. Previous research has determined that repeatability of a traditionally manufactured, injection molded LEGO® building block coupled with a LEGO® building block fabricated with the FDM process is between 2 and 10 μm, while the repeatability of two injection molded LEGO® building blocks coupled with one another is between 3 and 5 μm [16]. However, the impact of varying geometric parameters on the repeatability and accuracy of these FDM couplings has not been characterized.

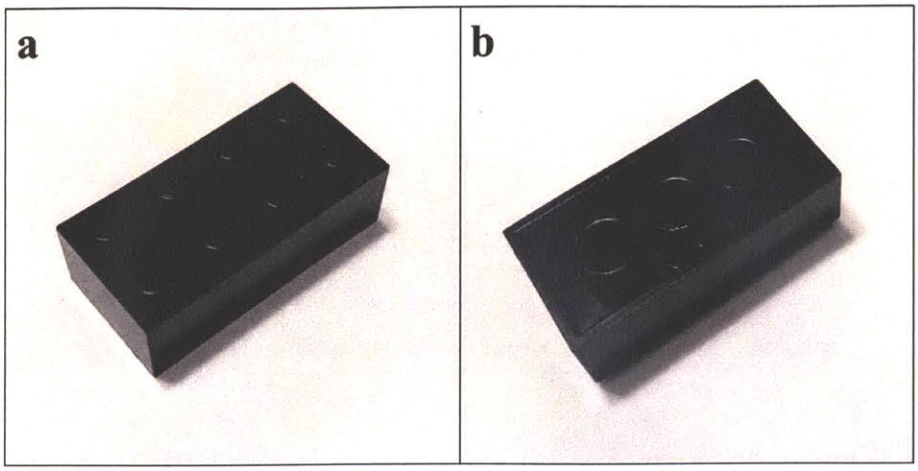

Figure 8. Lego building blocks. The a) pegs on top of one brick mesh with the b) thin web on the bottom of another brick

LEGO® building blocks are elastically averaged couplings because they use multiple contact areas between the pegs and web to improve the coupling accuracy. A well-designed, preloaded elastically averaged coupling, such as the LEGO® building blocks shown in Figure 8, has a repeatability that scales as $c * r/\sqrt{n}$, for a constant c, surface roughness r, and n contact points, indicating that the theoretical repeatability is a factor of $c/\sqrt{n}$ lower than the surface roughness of the individual layers, which, for FDM parts, is approximately 10-30 μm for a layer thickness of 0.254 mm (0.010 inches) [16,17].

Factorial Design of Experiments

The coupling variations tested in this research were designed using a factorial design of experiments in order to determine the trials necessary to determine the impact of varying coupling parameters on accuracy and repeatability. A factorial design of experiments (DOE) is used to characterize the trials necessary for determining the impact of multiple changing variables on a system. In a factorial DOE, the number of trials run is determined by the number of variables being tested and the number of levels for each variable, as shown in Equation 1, where n is the number of trials, k is the number of variables, and l is the number of levels for each variable. The levels are the different

values being tested for each variable. Note that in a factorial DOE, the number of levels must be the same for each variable, and 2 levels per variable are commonly used to determine the impact of each factor [18]. A sample scenario of 3 different factors, each with 2 levels, is shown in Table 3.

$$n = l^k \tag{1}$$

Table 3. Sample factorial DOE testing the impact of 3 factors, each with two levels, a low (-1) and a high (+1)

Trial	Factor 1	Factor 2	Factor 3
1	+1	+1	+1
2	-1	+1	+1
3	+1	-1	+1
4	-1	-1	+1
5	+1	+1	-1
6	-1	+1	-1
7	+1	-1	-1
8	-1	-1	-1

Compared to a one-factor-at-a-time DOE, in which one factor is varied at a time while the others are held constant, a factorial DOE requires fewer trials and is therefore more efficient [19]. In the example used in Table 3, with 3 factors, each with two levels, a one-factor-at-a-time DOE would require three times more trials than a factorial DOE.

EXPERIMENTAL APPARATUS AND PROCEDURE

The rendering of coupling used in this research is shown in Figure 9a-b, and the 3D printed coupling is shown in Figure 9c-d. The LEGO®-like interfaces were chosen because they form an elastically averaged coupling with key characteristics that are directly linked to certain dimensions. For example, the interference of the coupling can be directly altered by changing the diameter of the pegs. The coupling is circular to allow the Coordinate Measuring Machine (CMM) to utilize a pre-programmed circular path and determine the location of the center of the coupling. The base of the coupling, shown in Figure 9a, has raised pegs on the top surface, as well as an extrusion on the bottom surface used to clamp the coupling securely while taking measurements. The top of the coupling, shown in Figure 9b, has a web of thin-walled circular extrusions, supported with beams located between the extrusions. The fully coupled assembly rendering is shown in Figure 10a, and a 3D printed coupling is shown in Figure 10b. The 3D printed couplings were measured, and the peg heights were within 0.03 mm of the designed dimensions and the web diameters were within 0.01 mm of the designed dimensions.

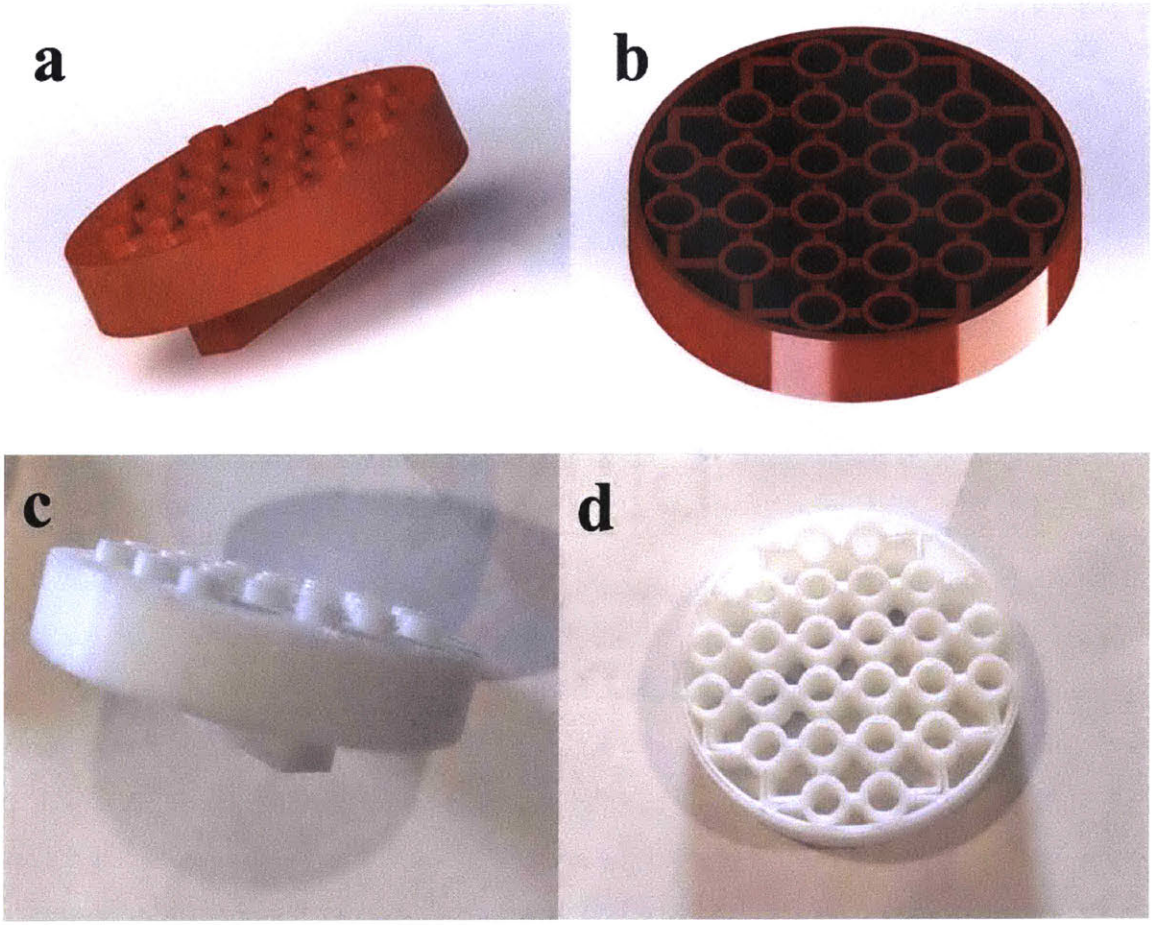

Figure 9. The renderings of the a) base and b) top of the coupling and the c) base and d) top of the printed coupling. The pegs on the top of the base fit between the circles on the bottom of the base.

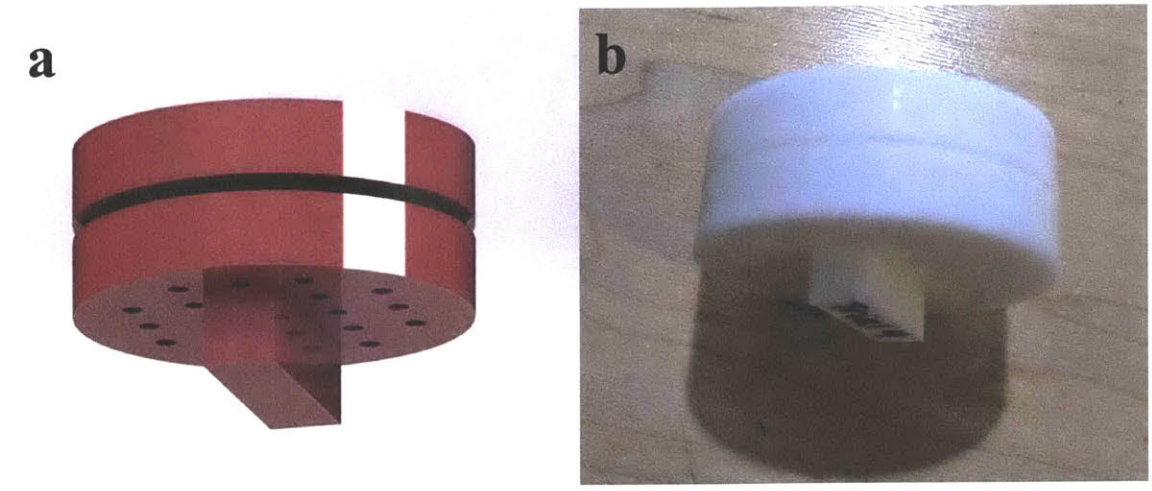

Figure 10. The a) rendering of the coupled assembly and b) 3D printed coupled assembly.

The interference of the coupling was changed by altering the web diameter of the top of the coupling, as shown in Figure 11a-b. The small web diameter of 6.25 mm corresponds to a smaller interference, and the large web diameter of 6.51 mm corresponds to a larger interference. By changing the interference, the number of contact points between the two halves of the coupling is varied by altering the deflection of the web by the pegs. The contact area of the coupling, defined as the area between the web and peg that touches between the two coupling halves, was changed by altering the peg height, as shown in Figure 11c-d. By changing the contact area, the number of contact points between the two halves is varied by altering the area where the pegs and web interact. The small peg height of 1.5 mm corresponds to a smaller contact area, and the tall peg height of 2.2 mm corresponds to a larger contact area. The stiffness of the coupling was changed with the addition of relief cuts to the web diameter on the top of the coupling, as shown in Figure 12. The lack of relief cuts corresponds to a higher stiffness, while the addition of relief cuts corresponds to a lower stiffness. By changing the stiffness, the compliance of the coupling interface is varied, and the force required to assemble the coupling is altered.

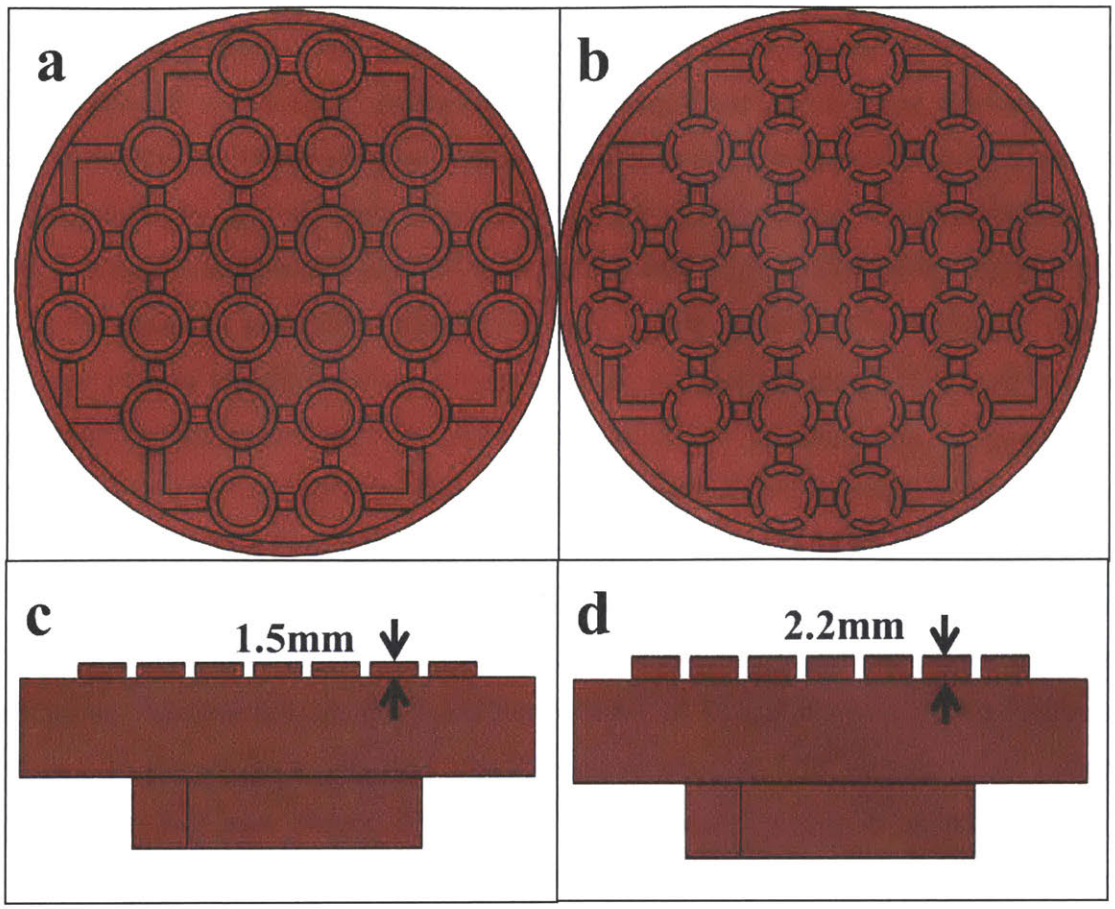

Figure 11. The a) small web diameter of 6.25 mm, b) large web diameter of 6.51 mm, c) short peg height of 1.5 mm, and the tall peg height of 2.2 mm.

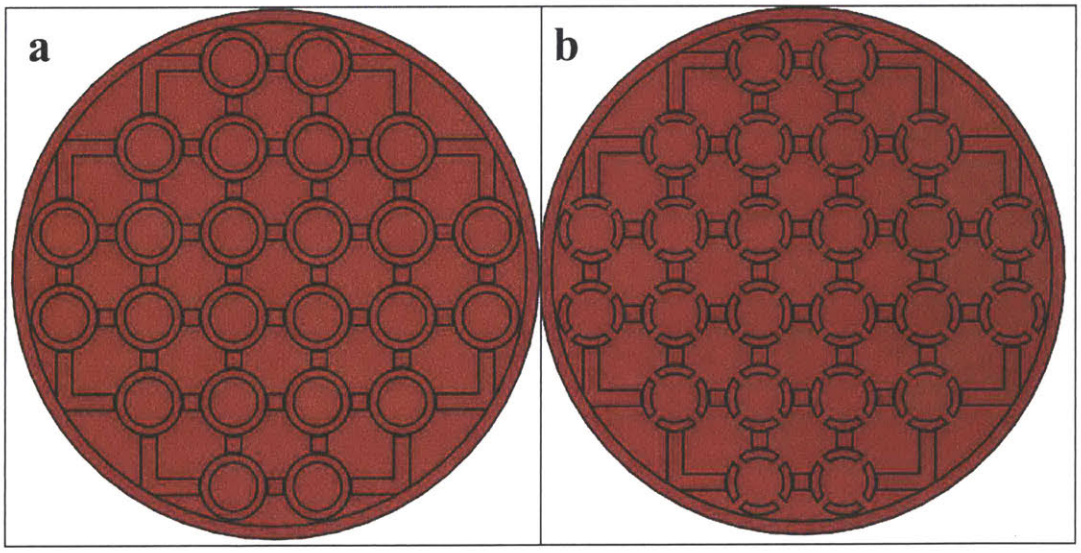

Figure 12. The coupling with a) no relief cuts and b) four relief cuts per web diameter.

A factorial design of experiments was used to design coupling variations that were measured to determine the impact of each parameter variation on the repeatability and accuracy of the coupling. The coupling variations used are shown in Table 4. A small interference indicates a reduction of the interference between the pegs of the base of the coupling and the web of the top of the coupling by 2% from the original design, requiring a web diameter of 6.25 mm, and a large interference indicates an increase of the interference by 2% from the original design, requiring a web diameter of 6.51 mm. The 2% change in web diameter results in a difference in interference that is significant enough to have an impact on the coupling accuracy and repeatability, but not so large that the interference is either so large that it prevents the coupling from being assembled or so small that the coupling halves do not contact each other. A small contact area indicates a reduction of the contact area between the pegs and the web by 20% from the original design, requiring a peg height of 1.50 mm, and a large contact area indicates an increase of the contact area by 20% from the original design, requiring a peg height of 2.20 mm. The 20% change in peg height results in a change in contact area that is significant enough to have an impact on coupling accuracy and repeatability, but not so large that the peg height is either so tall that the coupling cannot be assembled as designed or so small that the coupling halves do not have enough contact area to remain in an assembled state. A high stiffness indicates that there are no relief cuts in the web, and a low stiffness indicates that there are four relief cuts in the web.

Table 4. Coupling variations.

Variation	Interference	Contact Area	Stiffness
1	Small	Small	High
2	Large	Small	High
3	Small	Large	High
4	Large	Large	High
5	Small	Small	Low
6	Large	Small	Low
7	Small	Large	Low
8	Large	Large	Low

The coupling variations were printed using FDM on an Afinia H480 3D Printer in the orientation shown in Figure 13. This orientation was chosen because it resulted in the most accurate print and the smallest amount of support structures. The parts printed in this orientation are more accurate because the number of layers is minimized, and gravity has a smaller impact on accuracy than if, for example, the couplings were printed in this orientation rotated 90° about the x-axis. This orientation also minimizes the number of large overhangs and places all holes facing upwards, so there are fewer support structures necessary. The coupling variations were measured on a ZEISS MICURA Coordinate Measuring Machine (CMM) with Calypso software. The CMM has a resolution of 0.1 μm and is equipped with a VAST XT gold sensor and a ZEISS C99 controller, which enables scans of up to 200 measuring points per second [20]. As shown in Figure 14, an extrusion on the bottom of the base of each coupling variation was rigidly clamped onto the CMM table. To test for variation in the measurements due to the fixturing, the following procedure was executed:

1. Load the nominal geometry of the coupling (i.e., the CAD model) into the CMM software.
2. Fixture the base of the coupling, as shown in Figure 14.

3. Using the CMM probe, measure 3 points around the circumference of the base. This provides the CMM's analytical software a reference datum for the inspection.
4. Use the CMM circle program to probe the circumference of the base of the coupling, as shown in Figure 15a.
5. Place the top of the coupling onto the base and pre-load with 77 grams.
6. Use the CMM circle analysis routine to probe the circumference of the top coupling as shown in Figure 15b.
7. Using the CMM program, determine the radial misalignment between the base and top of the coupling using the data acquired.
8. Repeat steps 6-7, five times.

To determine the accuracy, characterized by the average radial misalignment of the coupling halves, and repeatability, characterized by the standard deviation of the radial misalignments, the following procedure was executed for each coupling variation:

1. Load the nominal geometry of the coupling (i.e., the CAD model) into the CMM software.
2. Fixture the base of the coupling, as shown in and Figure 14.
3. Using the CMM probe, measure 3 points around the circumference of the base. This provides the CMM's analytical software a reference datum for the inspection.
4. Use the CMM circle program to probe the circumference of the base of the coupling, as shown in Figure 15a.
5. Place the top of the coupling onto the base and pre-load with 77 grams.
6. Use the CMM circle analysis routine to probe the circumference of the top coupling as shown in Figure 15b.
7. Using the CMM program, determine the radial misalignment between the base and top of the coupling using the data acquired.
8. Remove the top of the coupling, place back onto the base of the coupling, and preload again with 77 grams.
9. Repeat steps 6-8, five times.

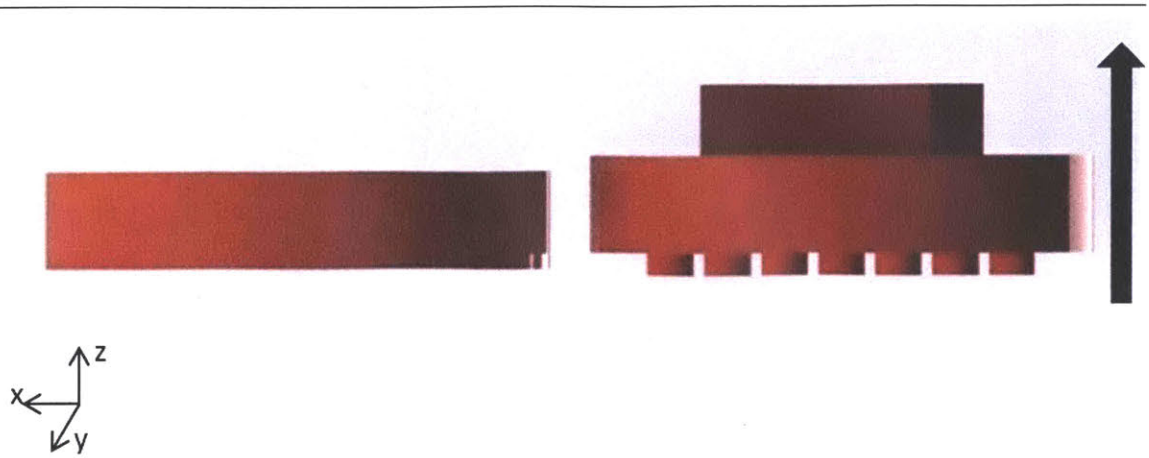

Figure 13. Print orientation and direction, indicated by the arrow.

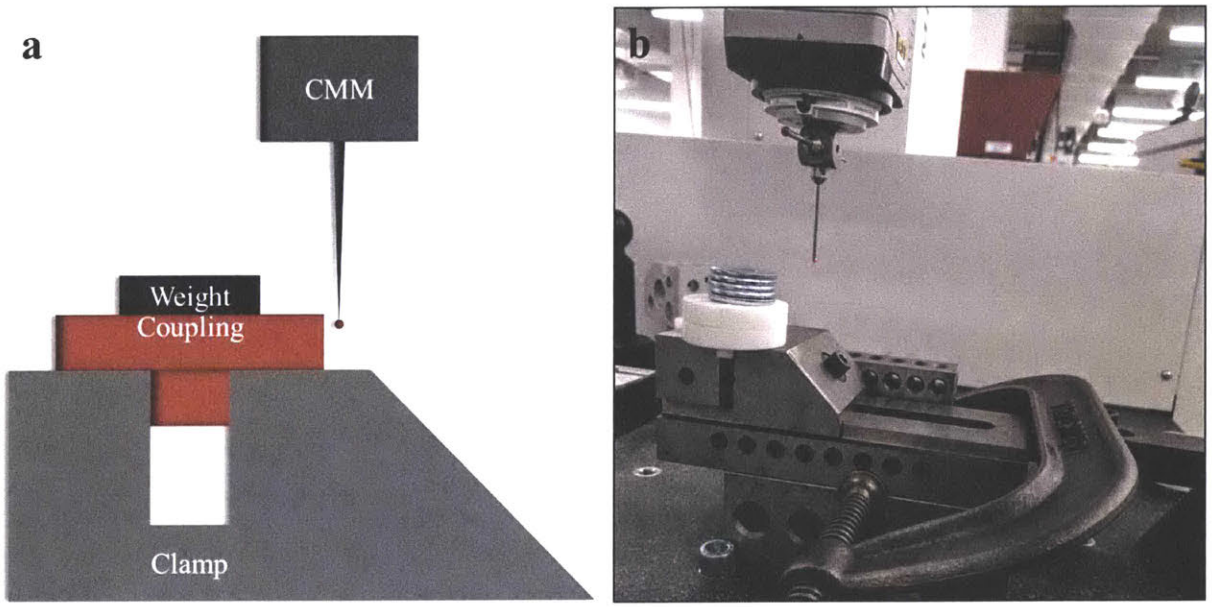

Figure 14. The a) modelled experimental setup and b) experimental setup.

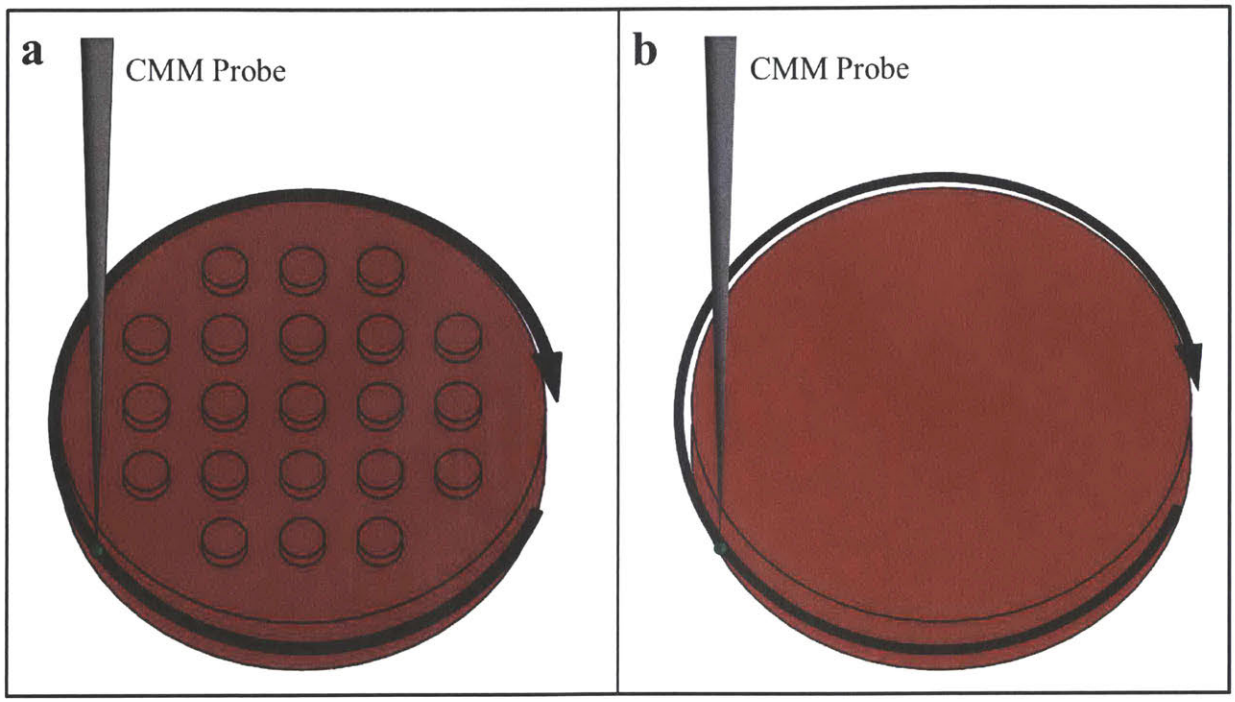

Figure 15. The path taken by the CMM to around the a) base of the coupling and b) top of the coupling to determine its location in space and dimensions.

To determine the accuracy and repeatability of each coupling variation, the CMM was used to measure radial misalignment between the base and top of the coupling, as shown in Figure 16. The CMM set the center of the base as the origin, and then calculated the distance from the origin to the center of the top. Thus, the misalignment is the scalar value of the 2D distance between the center of the lower component and the center of the upper component. The average of these measurements was used to indicate accuracy, so the more accurately the top of the coupling located onto the base of the coupling, the lower the average misalignment measurement would be. The standard deviation of these measurements was used to indicate repeatability; thus, a lower standard deviation indicates a more repeatable coupling assembly alignment.

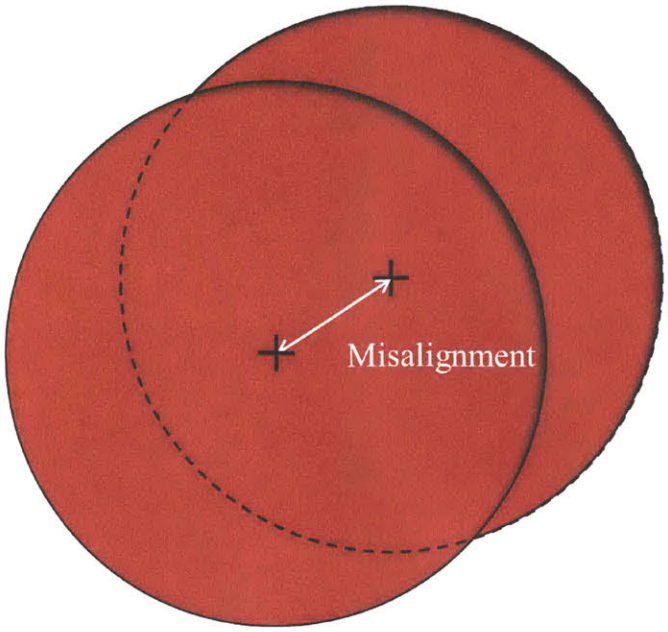

Figure 16. The distance between the centers of the base and top of the coupling used to determine misalignment.

The coupling was then imaged using tomography on a ZEISS Metrotom 800, using Metrotom OS 8.13280.0 to determine the points of contact between the web and pegs. These images were verified by covering the base of the coupling with ink, assembling the coupling, and visually inspecting the top of the coupling for places on the web where the ink had been transferred. The expected ink distribution is the distribution that occurs with traditionally manufactured LEGO® building blocks, shown in Figure 17. Ink spots can be seen on the top of the coupling where the pegs make contact with the webs when assembled. The ink spots indicate that the pegs contact each circle in the web at 45°, 135°, 225°, and 315°, shown in Figure 18.

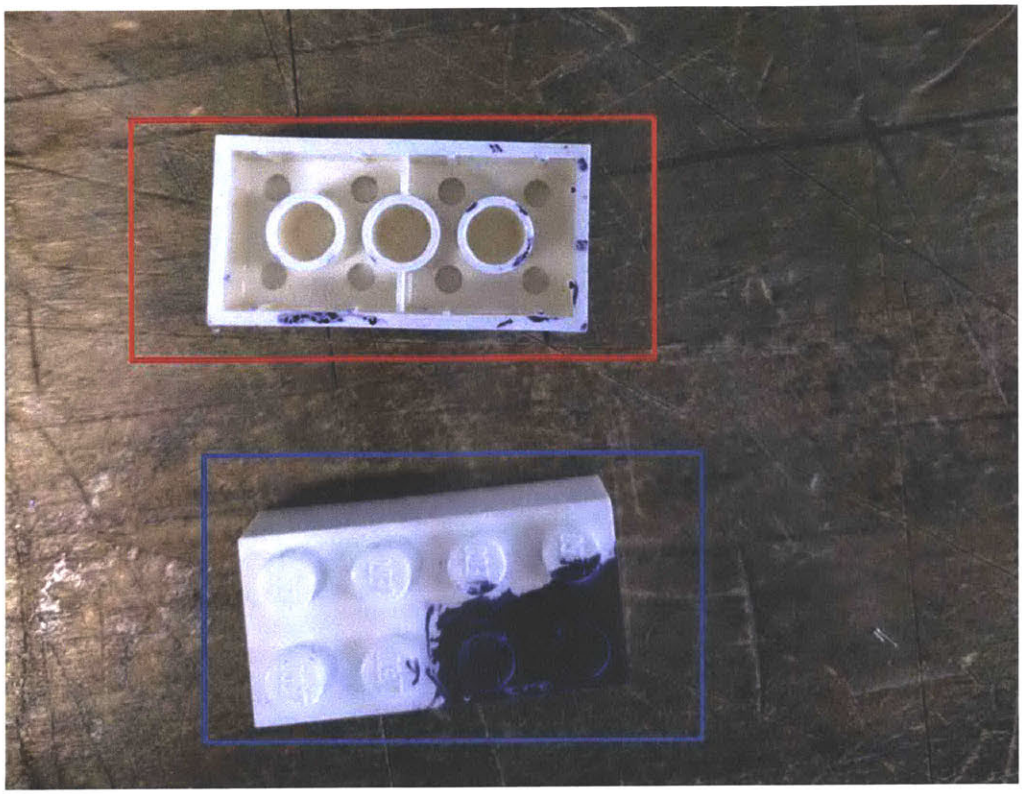

Figure 17. The ink distribution on traditionally manufactured LEGO® building block. The circular web on the top of the coupling, boxed in red, shows inked spots 90° apart from each other, indicative of the locations where the ink-covered pegs of the base coupling, boxed in blue, made contact.

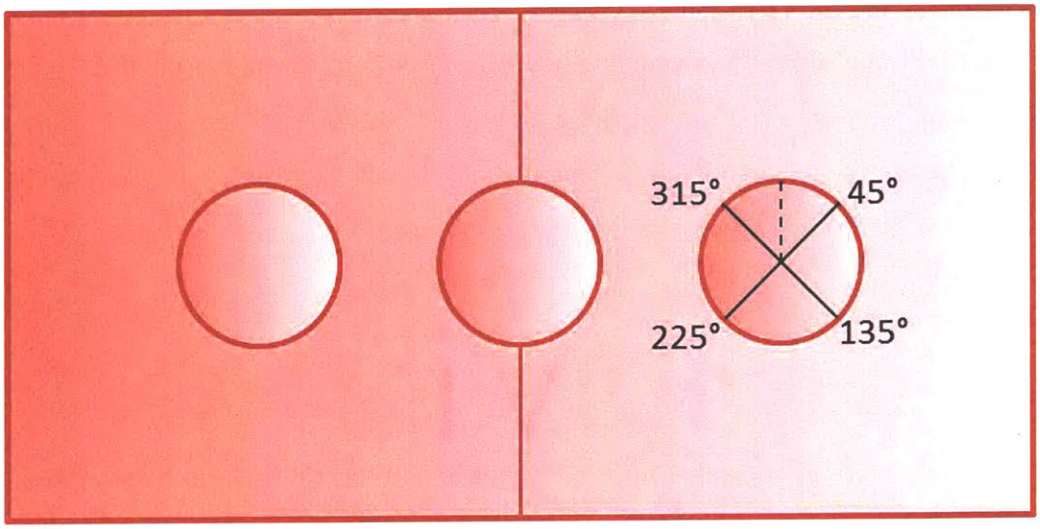

Figure 18. The points at which the pegs contact the web on a traditionally manufactured LEGO®.

RESULTS AND DISCUSSION

The repeatability of the fixturing setup, indicating how well the clamp holds the coupling in place, was found to be 0.16 μm. This value is approximately 5% of the value found for the repeatability of the coupling variations, indicating that the method of fixturing did not have a significant impact on the result of the coupling variation measurements.

For each of the trials listed in Table 4, 5 measurements of the misalignment between the base and the top of the coupling were taken, as shown in Figure 16, and Table 5 lists the averages and standard deviations of these measurements for each coupling variation.

Table 5. Misalignment averages and standard deviations for each coupling variation.

Variation	Average of Misalignment Measurements (μm)	Standard Deviation of Misalignment Measurements (μm)
1	17.85	3.96
2	8.38	3.86
3	15.44	3.17
4	11.00	5.49
5	10.99	5.92
6	17.22	3.64
7	10.02	3.20
8	10.23	2.53

Accuracy

The accuracies of the coupling variations, indicated by the average misalignment of the top and base of the coupling, are shown in Figure 19. The accuracy of the couplings with varied contact is shown in red. The small contact corresponds to a peg height of 1.5 mm, and the large contact area corresponds to a peg height of 2.2 mm, as shown in Figure 11c-d. The couplings with a smaller contact area were 1.97 μm, or 17%, less accurate than couplings with a larger contact area.

The accuracy of the couplings with varied interference is shown in blue. The small interference corresponds to a web diameter of 6.25 mm, and the large interference corresponds to a web diameter of 6.51 mm, as shown in Figure 11a-b. The couplings with larger interference were 1.86 μm, or 16%, less accurate than couplings with smaller interference.

The accuracy of the couplings with varied stiffness is shown in purple. The low stiffness corresponds to a web with no relief cuts, and the high stiffness corresponds to a web with four relief cuts, as shown in Figure 12. The couplings with a higher stiffness were 1.06 μm, or 8%, less accurate than couplings with a lower stiffness.

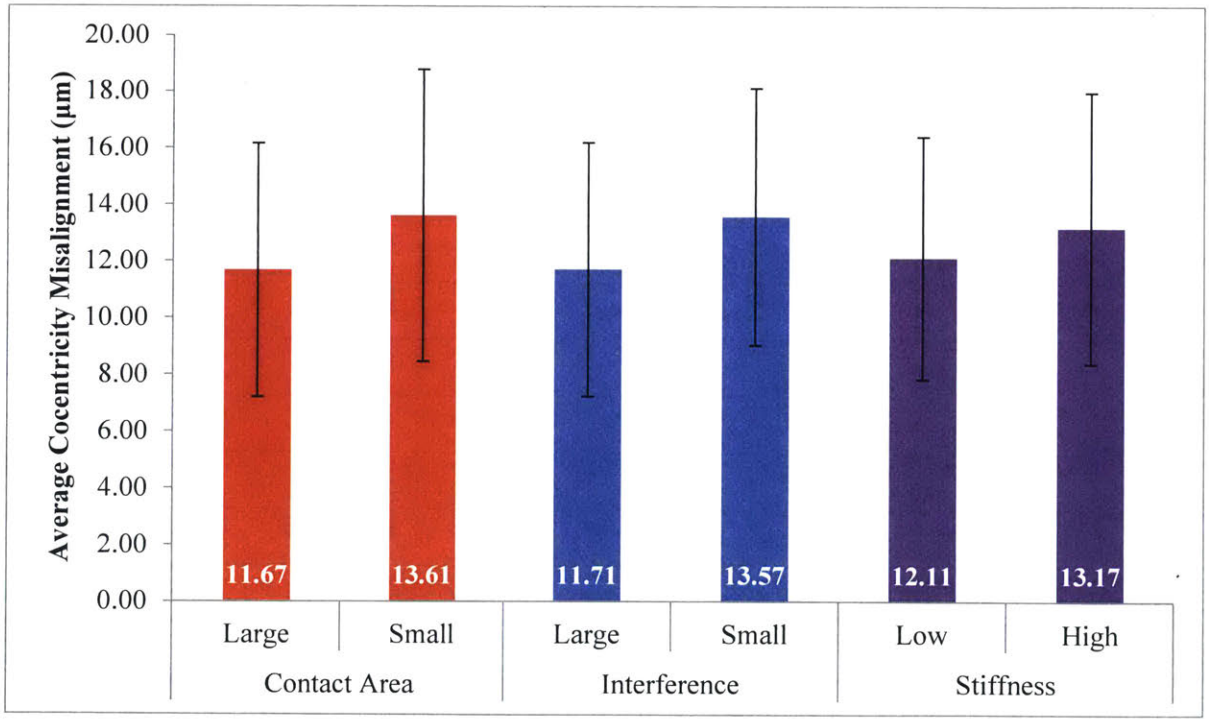

Figure 19. Accuracies of the couplings with contact area, interference, and stiffness varied, with 95% confidence bars

Repeatability

The repeatabilities of the coupling variations, indicated by the standard deviations of the misalignments of the top and base of the coupling, are shown in Figure 20. The repeatability of the couplings with varied contact area is shown in red. The small contact

corresponds to a peg height of 1.5 mm, and the large contact area corresponds to a peg height of 2.2 mm, as shown in Figure 11c-d. The couplings with a smaller contact area were 0.75 μm, or 15%, less repeatable than couplings with a larger contact area.

The repeatability of the couplings with varied interference is shown in blue. The small interference corresponds to a web diameter of 6.25 mm, and the large interference corresponds to a web diameter of 6.51 mm, as shown in Figure 11a-b. The couplings with less interference were 0.06 μm, or 1%, less repeatable than couplings with more interference.

The repeatability of the couplings with varied stiffness is shown in purple. The low stiffness corresponds to a web with no relief cuts, and the high stiffness corresponds to a web with four relief cuts, as shown in Figure 12. The couplings with a higher stiffness were 0.57 μm, or 12%, less repeatable than couplings with a lower stiffness.

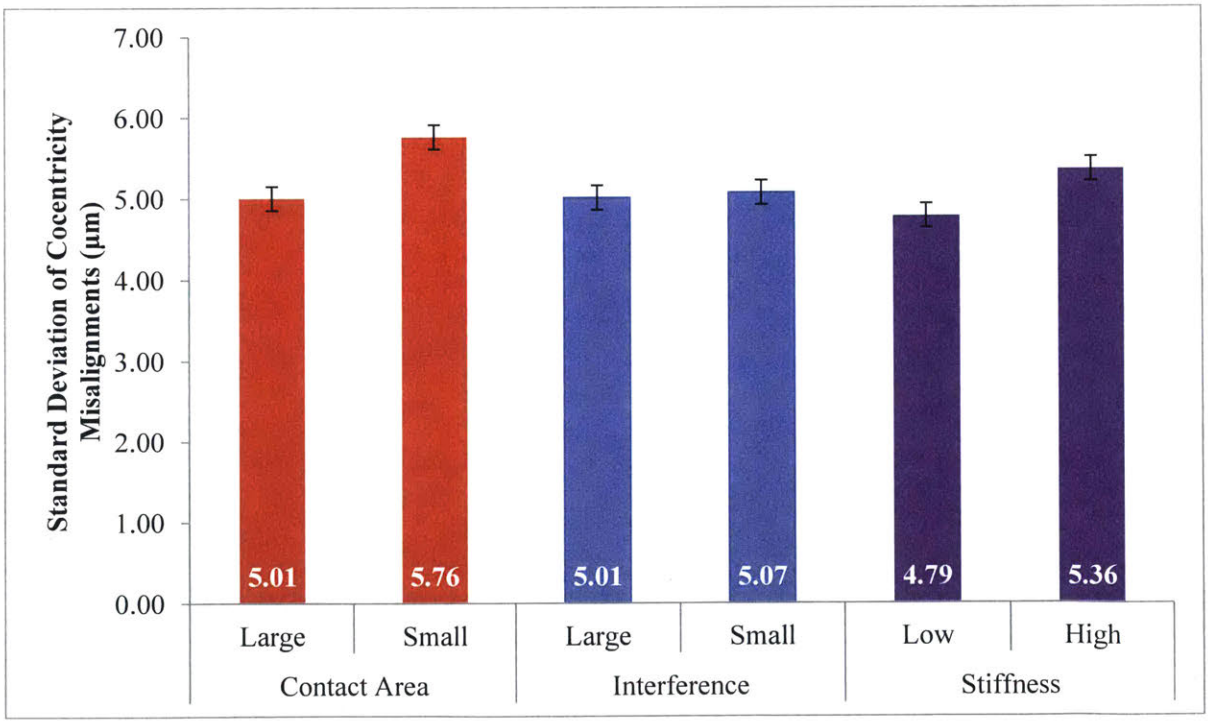

Figure 20. Repeatabilities of the couplings with contact area, interference, and stiffness varied, with bars indicating 95% confidence of the fixturing setup.

Contact Points

The repeatability of the couplings was not as good as predicted by the relationship between the repeatability and the number of contact points within the coupling. When the assembled coupling was imaged with tomography, the coupling appeared to have fewer contact points than expected. As shown in Figure 21, there are only three contact points, instead of 4 contact points around each peg where it touches the web. Because the number of contact points is lower than expected, the repeatability is not as good as predicted.

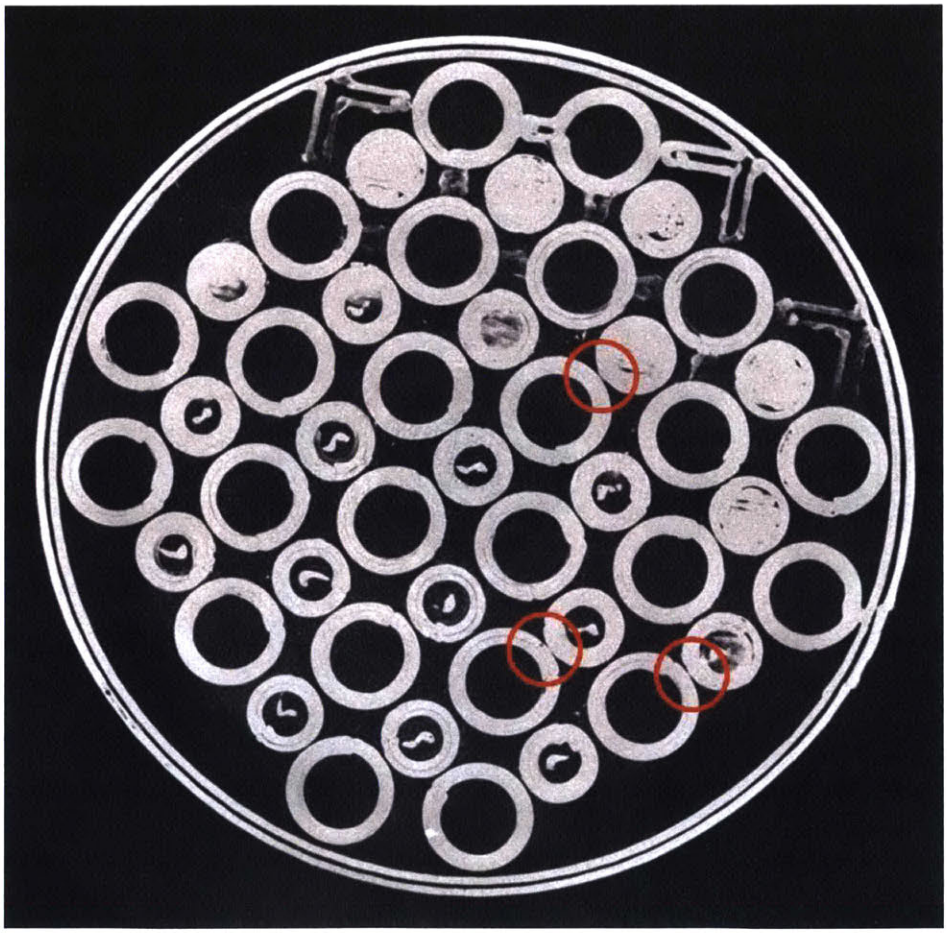

Figure 21. Assembled coupling as imaged with tomography, with contact points circled in red.

The tomography imaged was verified by determining where ink applied to the base of the coupling transferred to the top of the coupling when the two parts were paired, as shown in Figure 22. Instead of the expected ink distribution of four inked spots

per circle in the web, shown in Figure 17, the ink was distributed unevenly, and some of the circles received no ink at all. The difference between the expected ink distribution and the actual ink distribution confirmed that the number of contact points within the coupling was less than expected.

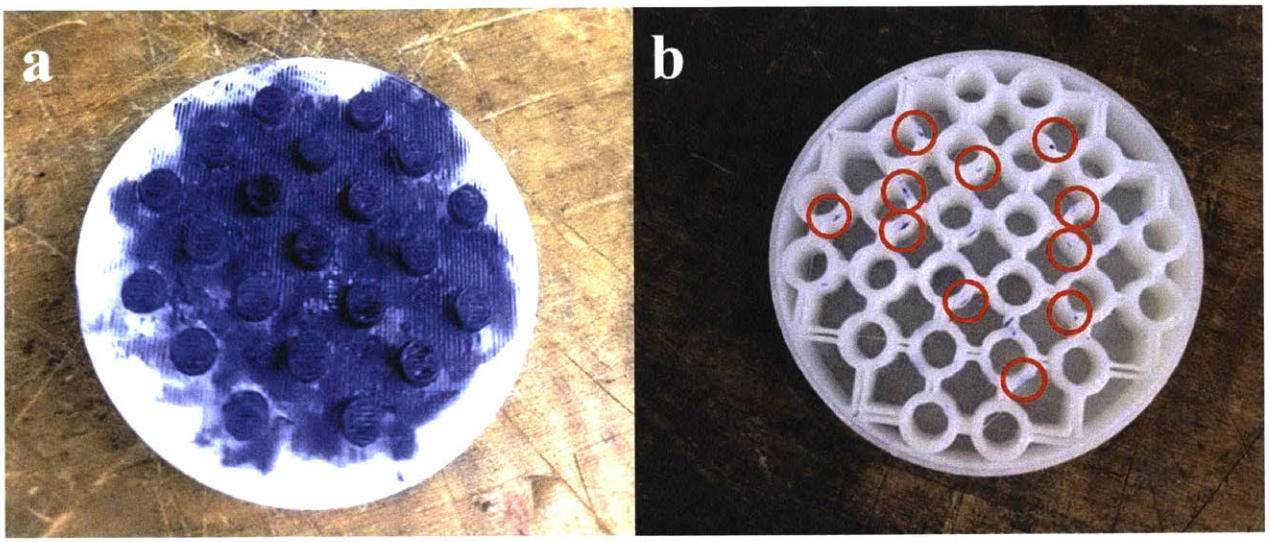

Figure 22. The a) base of the coupling, with ink applied to the pegs, and b) the top of the coupling, with the areas of ink transfer circled in red.

Discussion

The effect of varying parameters on the accuracy of the couplings is statistically insignificant, as the differences in accuracies are small enough and the errors of the accuracies are large enough that the errors overlap. The effect of varying interference on repeatability was also statistically insignificant, but the effects of varying contact area and stiffness on repeatability were statistically significant.

A reduction in contact area of 40% decreased repeatability by 15%. Decreasing contact area lowers the number of contact points between the two coupling halves, so the total error increases. Increasing stiffness decreased repeatability by 12%. An increased stiffness causes the web to become less compliant, and the force necessary to couple two coupling halves with a higher stiffness is greater than the force necessary to couple two coupling halves with a lower stiffness. The pre-load used for each coupling variation

remained constant, so the couplings with an increased stiffness did not have a corresponding increase in pre-load and were therefore less repeatable.

CONCLUSIONS AND RECOMMENDATIONS

Key parameters of a LEGO®-like coupling, including contact area between coupling halves, interference between coupling halves, and stiffness of the web, were varied in a factorial design of experiments. The coupling variations were tested for accuracy and repeatability by determining the average radial misalignment and the standard deviation of the radial misalignment measurements taken after decoupling and recoupling each coupling. The couplings were displayed accuracy on the order of 10 μm and repeatability on the order of 1 μm. This research determined that varying interference, contact area, and stiffness had a statistically insignificant effect of accuracy. Varying interference had a statistically insignificant effect on repeatability, increasing contact area increased repeatability by 0.75 μm, or 15%, and increasing increased repeatability by 0.57 μm, or 12%.

Further optimization of each parameter would require varying each parameter more than two times in order to quantify any relationships between the parameter and the repeatability and accuracy of the couplings. The influence of the varied parameters on each other should also be determined by comparing paired statistics. Further trials should also make use of a larger preload to ensure that the coupling halves mesh together as designed.

The number of contact points between the base and top of the coupling was lower than expected, especially in couplings with a low interference. This number could be improved by increasing the web diameters, which would also require a higher preload to ensure the two coupling halves assemble correctly. The tomography image in Figure 21 shows the point on each circle on the top of the coupling where the 3D printer started and finished its extrusion, and contact points tended to occur more frequently closer to these points because these points are wider than the rest of the circle. In the future, the print pattern followed by the 3D printer to create these circles should be oriented such that the extra thickness around the starting point does not impact the contact between the base and top of the coupling.

To further study the impact of the AM process on the couplings, multiple prints of the same coupling could be fabricated and tested for repeatability and accuracy, as material properties of AM parts are not well controlled at this time. Tomography could be

used to observe and characterize the accuracy of the print of the pegs and webs, including verifying the dimensions of the parts and the circularity of the pegs and webs. Tomography could also be used to determine the actual number of contact points within the coupling when assembled, which would allow for more accurate relationships between the number of contact points and the accuracy and repeatability of the coupling.

The accuracy and repeatability of the couplings are good enough to justify the use of these AM LEGO®-like couplings to enable multi-part AM assemblies. To enable multi-part AM assemblies that do not require a preload to remain in an assembled state, the interference of the couplings could be increased more than the 2% increase explored in this research. A higher interference would require a higher force to assemble the coupling initially, but once assembled, the coupling halves would not require a constant load to remain together, similarly to traditionally manufactured LEGO® building blocks. Before these AM couplings are used in assemblies in which precision locating is critical, more trials should be run to quantitatively characterize the relationships between the parameters varied and the accuracy and repeatability of the couplings.

BIBLIOGRAPHY

[1] Slocum, A., 2010, "Kinematic Couplings: A Review of Design Principles and Applications," Int. J. Mach. Tools Manuf., **50**(4), pp. 310–327.

[2] Willoughby, P., 2005, *Elastically Averaged Precision Alignment.*, c2005.

[3] "ASTM Standard F2792-12a, 2012, 'Standard Terminology for Additive Manufacturing Technologies,' ASTM International, West ."

[4] Phillips, W. H., 2016, *Additive Manufacturing : Opportunities, Challenges, Implications*, Nova Science Publishers, Inc, New York.

[5] Shubham, P., pshubham@amity.ed., Sikidar, A., arnab.sikidar@gmail.co., and Chand, T., tegchandsoni@gmail.co., 2016, "The Influence of Layer Thickness on Mechanical Properties of the 3D Printed ABS Polymer by Fused Deposition Modeling.," Key Eng. Mater., **706**, pp. 63–67.

[6] "Compare MakerBot Replicator Printers | MakerBot" [Online]. Available: https://www.makerbot.com/compare-3d-printers/. [Accessed: 27-Apr-2017].

[7] "Dell Search" [Online]. Available: http://pilot.search.dell.com/makerbot%20printer. [Accessed: 27-Apr-2017].

[8] Crump, S. S., 1992, "Apparatus and Method for Creating Three-Dimensional Objects."

[9] Crump, S. S., 1996, "Process of Support Removal for Fused Deposition Modeling."

[10] "How Does Part Orientation Affect a 3D Print?," 3D Hubs [Online]. Available: https://www.3dhubs.com/knowledge-base/how-does-part-orientation-affect-3d-print. [Accessed: 02-May-2017].

[11] "Afinia H480 3D Printer (Discontinued)," Afinia 3D Print.

[12] Culpepper, M. L., Slocum, A. H., Shaikh, F. Z., and Vrsek, G., 2003, "Quasi-Kinematic Couplings for Low-Cost Precision Alignment of High-Volume Assemblies," J. Mech. Des., **126**(3), pp. 456–463.

[13] "Kinematic Couplings" [Online]. Available: http://pergatory.mit.edu/kinematiccouplings/html/about/elastic_averaging.html. [Accessed: 21-Dec-2016].

[14] "Kinematic Coupling for Precision Fixturing and Assembly.pdf."

[15] Slocum, A. H., and Donmez, A., 1998, "Kinematic Couplings for Precision Fixturing - Part 2: Experimental Determination of Repeatability and Stiffness," Precis. Eng., **10**(3).

[16] Owens, C., 2017, "Modular LEGO Brick Microfluidics," Massachusetts Institute of Technology.

[17] Nourghassemi, B., 2011, "Surface Roughness Estimation for FDM Systems," Ryerson University.

[18] "5.3.3.3.2. Full Factorial Example" [Online]. Available: http://www.itl.nist.gov/div898/handbook/pri/section3/pri3332.htm. [Accessed: 08-May-2017].

[19] Hicks, C. R., and Turner, K. V., 1999, *Fundamental Concepts in the Design of Experiments*, Oxford University Press.

[20] "ZEISS MICURA CMM - Precision for Small Parts" [Online]. Available: https://www.zeiss.com/metrology/products/systems/bridge-type-cmms/micura.html. [Accessed: 04-May-2017].